Zonal and Seasonal Variations of the Near-Surface Heat Balance of the Equatorial Pacific Ocean

DAVID B. ENFIELD

College of Oceanography, Oregon State University, Corvallis, OR 97331

(Manuscript received 26 March 1985, in final form 25 November 1985)

ABSTRACT

This study calculates a detailed climatological inventory of the oceanic heat balance in the equatorial Pacific. The gridded climatology of Weare et al. is used as an estimate of net surface heating. Zonal and meridional/vertical advection are estimated in a manner similar to that of Wyrtki, using the gridded climatologies for wind stress (Wyrtki and Meyers) and sea surface temperature (Reynolds), plus estimates of zonal transport. In addition, the meridional diffusion of heat into the cold tongue has been estimated from the work of Hansen and Paul and the terms of the heat balance have been resolved by ten-degree longitude zones and by month of the year. The computed residual heat flux has been examined for consistency with expectations about the remaining, vertical diffusion process. The effects of using the alternate climatologies of Esbensen and Kushnir and Reed for the net surface heating are also calculated.

The total advective heat flux divergence is calculated to be -27 ± 7, -91 ± 17 and -48 ± 17 W m^{-2}, respectively, in the western, central and eastern equatorial Pacific with meridional advection and upwelling removing about three times as much heat as zonal advection. The advective contributions are in approximate agreement with Wyrtki's "likely case" estimates for the 100°W–170°E longitude zone. The contributions from zonal advection, meridional advection and meridional diffusion are found to be greatest during the Boreal fall, winter and fall–winter seasons, respectively.

Depending on the climatology used for the net surface heat gain, the assumption of a uniform meridional diffusivity of 2×10^4 m^2 s^{-1} leads to physically unrealistic residual flux divergences that imply a heat gain from vertical turbulence in the central Pacific or that vertical turbulence removes much more heat from the western and eastern Pacific than from the central Pacific. Total neglect of the meridional diffusion exacerbates the problems. Increasing the meridional diffusivity to 6×10^4 m^2 s^{-1} in the central Pacific, consistent with direct estimates by Hansen and Paul, gives zonally uniform, negative residuals that are physically consistent with existing measurements of equatorial turbulence. With the model so tuned, the "best guess" heat balance in the central Pacific involves significant contributions from all terms, in the western Pacific between surface heat gain from the atmosphere and losses due to vertical diffusion, and in the eastern Pacific between surface gain and losses due to meridional advection (upwelling) and vertical diffusion.

1. Introduction

One of the principal thrusts of present and future research in oceanography is aimed at understanding the role played by oceanic heat transports in controlling global climate over time scales useful for prediction (Webster, 1984). An area of primary importance to such studies is the equatorial Pacific, where the time scale of the basin response to forcing by the trade winds permits an aperiodic, interactive feedback between the ocean and the overlying atmosphere with the consequent growth and persistence of positive sea surface temperature (SST) anomalies known as the El Niño (Cane, 1983). These in turn provide an anomalous heat source that is thought to drive persistent circulation and weather anomalies in the global atmosphere (Rasmusson and Wallace, 1983), with important economic consequences in widely separated regions of the world. The problem, for the oceanographer, is one of understanding 1) the processes that govern the normal thermal characteristics of the equatorial ocean, and 2) how their balance is altered during anomalous episodes. The former task is a prerequisite to the latter and is the subject of this paper.

Unfortunately, too little is known about the various contributions to the heat budget. Estimates for the net heat gained from the atmosphere by the equatorial Pacific Ocean vary from 50 W m^{-2} to 110 W m^{-2}. Over most of this range our present calculations of the heat removed by the ocean through advection exceed the surface gain, implying a deficit (Wyrtki, 1981). The discrepancy, if real, means that diffusive fluxes play a significant role. The purpose of this paper is to assemble as much of the existing information as possible into a carefully constructed budget from which some tentative conclusions can be formed and research strategies suggested.

In studying the equatorial heat balance it is particularly useful to resolve the climatology both zonally and seasonally. Zonal and annual variations occur in winds, currents and temperature gradients that will change the relative contributions of the various heat

flux terms to the overall balance, depending on the longitude sector and season examined. These variations must be accounted for in trying to understand the magnitude and timing of thermal anomalies that accompany El Niño episodes (e.g., Harrison and Schopf, 1984). Moreover, in studies such as this, where large systematic and random errors exist in the data, one gains added confidence in the estimation of factors that are important to the overall heat balance when their spatial and seasonal variations match with expectations. Lastly, because the data inputs used to calculate many of the component heat budget terms combine nonlinearly, it is advisable to do the computations for smaller time–space units and integrate the results to the scales desired.

The next section reviews previous work to establish the starting point and conceptual model for later sections, which calculate and discuss in turn the zonal and seasonal behavior of the heat balance components that are most amenable to estimation: advection by mean flows plus meridional diffusion. Uncertainties in the oceanic terms are estimated and the residual heat flux unaccounted for is then examined for consistency with the remaining component—vertical diffusion by turbulent mixing.

2. The equatorial Pacific heat balance

Over the long term and away from continental boundaries, most of the net interfacial exchange of heat between the ocean and atmosphere (Q_n) is balanced within the ocean by the heat flux divergence due to horizontal advection across isotherms. The equatorial heat balance, however, is more complex. In equatorial regions, for example, the zonal and meridional components of the advective flux divergence are typically treated separately for reasons of symmetry and because different dynamics are involved. The zonal component (Q_u) results from the westward advection of cool water by the South Equatorial Current (SEC), while the meridional component (Q_v) arises from the action of steady easterly winds in producing poleward Ekman transports away from the equator, a process that is also primarily responsible for vertical advection (equatorial upwelling).

Diffusive fluxes may also contribute significantly to the equatorial heat balance. The total disappearance of Coriolis effects at the equator allows for the existence of the strong Equatorial Undercurrent (EUC), which transports water eastward in partial compensation for near-surface water that is transported westward by the SEC. The vertical juxtaposition of the two flows results in a strong vertical shear that makes eddy kinetic energy available for the diffusive exchange of heat between the upper and lower layers ($Q_{d,z}$), in addition to that provided directly by the wind.

The lateral eddy diffusion of heat may also be important, and here again the zonal and meridional components ($Q_{d,x}$, $Q_{d,y}$) are treated separately. The meridional eddy diffusion is most likely to be significant where a strong north–south shear between zonal currents coincides with a large meridional temperature gradient, as in the central equatorial Pacific (Philander, 1976, 1978). Zonal SST gradients, however, are at least an order of magnitude smaller and zonal shears are insignificant in comparison. If the zonal diffusion term is ignored, the spatial integration of the governing equation for heat gives

$$Q_h = (Q_u + Q_v + Q_{d,y} + Q_{d,z}) + Q_n, \qquad (1)$$

where Q_u and Q_v both involve the effects of vertical as well as horizontal advection and all terms are treated as positive when they represent gains to the ocean. The term Q_h on the left side of (1) is the time rate of change of heat content, or the *heat storage rate* as used by Levitus (1984).

Wyrtki (1981) uses long-term climatological means of SST, winds and hydrographic data to estimate annual mean values for Q_u and Q_v within a 50 m thick surface layer bordered by meridional boundaries at 5°N and 5°S and by zonal boundaries at 100°W and 170°E. Wyrtki assumes an average surface heat gain of $Q_n = +85$ W m^{-2} and, by definition, Q_h is zero in his time-averaged calculation. Using the observed zonal SST gradient and assuming an average SEC flow through the volume of -27 cm s^{-1}, he estimates that horizontal advection removes heat at the rate of $Q_u = 3.8 \times 10^{-14}$ W. His calculation of 8.4×10^{-14} W for Q_v is based on an estimated average SST difference of 4°C between the base of the box and the meridional boundaries, and on poleward Ekman transports computed from the Wyrtki and Meyers (1976) zonal wind stress climatology combined with an equatorward geostrophic transport estimates from dynamic height data near the zonal boundaries. Wyrtki estimated $Q_{d,y}$ to be negligible, based on his assumption of a meridional eddy diffusivity of $K_y = 10^3$ m^2 s^{-1} (typical of most open ocean regions). He also calculates a negligible value for $Q_{d,z}$, based on a vertical eddy diffusivity of $K_z = 2 \times 10^{-6}$ m^2 s^{-1} within 100 km of the equator and $K_z = 10^{-6}$ m^2 s^{-1} elsewhere.

As Wyrtki points out, a heat deficit results from the above calculations, with about 40% more heat exported out of the volume by the oceanic advection than is gained from the atmosphere. To achieve a balance he arrives at a modified "likely case" by reducing the estimated zonal transport as well as the difference in temperature between the upwelling water and that transported through the meridional boundaries. Wyrtki concludes that the latter is only reasonable if the upwelling is a shallower process than previously assumed. The work of Bryden and Brady (1985), however, suggests that the upwelling process is not confined to the surface layer. Hence, the discrepancy found by Wyrtki appears to remain unresolved.

It is possible, of course, that the balance is not simply

one between surface heat gain and advective transports. Work by Niiler and Stevenson (1982) and Hansen and Paul (1984) indicates that the vertical and meridional diffusive fluxes are not negligible in equatorial regions as estimated by Wyrtki (1981). The relative contributions of these diffusive fluxes are important to understand: they remove and add heat from/to the equatorial cold tongue, respectively. Hence, they are not additive and their combined contribution to the balance is not clear.

3. Model geometry and data overview

I should point out that the complementary work of others (e.g., Niiler and Stevenson, 1982; Bryden and Brady, 1985) involves methods that are not appropriate to the specific task here, though they do enjoy inherent analytical advantages. Thus, by examining the time-averaged balance within the pools of water warmer than 28° or 26°C in the tropical Atlantic and Pacific, Niiler and Stevenson (1982) were able to eliminate the uncertain effects of advection and focus on the diffusive processes. This is not appropriate where time-invariance cannot be assumed, as in the season-resolving approach of this paper. Moreover, attention to a given isotherm results in a model that excludes much of the eastern Pacific, while in the central and western Pacific it extends to latitudes considerably beyond ±5° and thus obscures processes that are unique to the equatorial zone. The study by Bryden and Brady (1985) is successful in clarifying the role of processes below the equatorial surface layer but is limited in its seasonal and zonal resolution due to the scarcity of subsurface data. In order to preserve the zonal extent and equatorial nature of the calculations and at the same time avoid the need for detailed information on the behavior of temperature and currents with depth, it is necessary to consider a shallow volume above the thermocline and below the Ekman layer, as Wyrtki (1981) has done. In this study, however, we refine Wyrtki's calculations by including diffusive fluxes, resolving the model zonally and seasonally and by using the most recent gridded climatologies of surface flux and SST. The strategy is to estimate all terms in (1) except for the vertical diffusion ($Q_{d,z}$), which is "modeled" by the residual in the calculations and can be examined for its consistency with present knowledge.

In this analysis I have kept Wyrtki's (1981) 5°N–5°S meridional extent, but have resolved the calculations zonally into 13 successive 10° × 10° boxes from 150°E to 80°W (Fig. 2). Shading is used in Fig. 2 to indicate the longitude subrange over which Wyrtki made his calculations. For purposes of comparison, integrated values for the shaded region will frequently be cited. References to the western, central and eastern Pacific are taken to mean the 150°E–170°W, 170°W–120°W and 120°W–80°W longitude zones, respectively. To ensure the relative uniformity of temperature within the near-surface volume being analyzed, the vertical extent of each box is decreased east of 140°W to accomodate the shrinking mixed layer. The minimum box thickness of 20 m is found along 80°–110°W. While this is uncomfortably close to the base of the Ekman layer and the depth limit for short-wave penetration, large errors would result from allowing the boxes to extend into the thermocline. The computations require monthly gridded climatological summaries of three fields: the net downward heat flux at the surface (Q_n) by Weare et al. (1981b), the zonal wind stress (τ^x) by Wyrtki and Meyers (1976) and the sea surface temperature by Reynolds (1982). In addition, one must estimate the zonal and annual variations of the average zonal current (U) in a way that is consistent with direct measurements that have been made. In order that surface fluxes and oceanic fluxes be easily compared, all heat fluxes are standardized in terms of the equivalent rate of heat transfer through a unit area of sea surface (W m^{-2}).

4. SST and heat storage rate

The monthly climatological SST summary of Reynolds (1982) was used for this study because it combines thoughtful processing of the surface marine dataset with a relatively fine scale spatial definition of thermal features. The latter is needed to resolve the temperature gradients used in the calculations of the meridional fluxes. In the original preparation of the SST climatology, the 1° × 1° gridded data were spatially smoothed with a running median filter spanning four grid points, giving the data an effective resolution of about 200 km (Reynolds, personal communication, 1985).

Examples of the SST data in the tropical Pacific are shown in Fig. 1 for the climatically extreme months of March and September. Note, in particular, how the data are able to resolve the relatively narrow coastal upwelling zone off Peru. The equatorial upwelling zone in the eastern and central Pacific is also clearly evident. The latter feature shows a strong annual variation, being best developed in September between the Galapagos (90°W) and Line Islands (155°W). Note also the north–south asymmetry, with the strongest temperature gradient found north of the equator and the temperature minimum just south of the equator.

The 1° × 1° SST data were averaged into single values for the 10° × 10° boxes centered on the equator (Fig. 3) and the heat storage rate was calculated as $Q_h = \rho C_p H(x) \cdot (\Delta T/\Delta t)$, where ρ is the water density, C_p the specific heat, $H(x)$ the box thickness and $\Delta T/\Delta t$ the time rate of change of the box temperature, figured by centered differences in time.

The temperature is assumed to be uniform at the surface value throughout each box. This is not strictly true, of course. In the central Pacific the temperature at 50 m is typically about 0.5–1.0°C cooler than at the

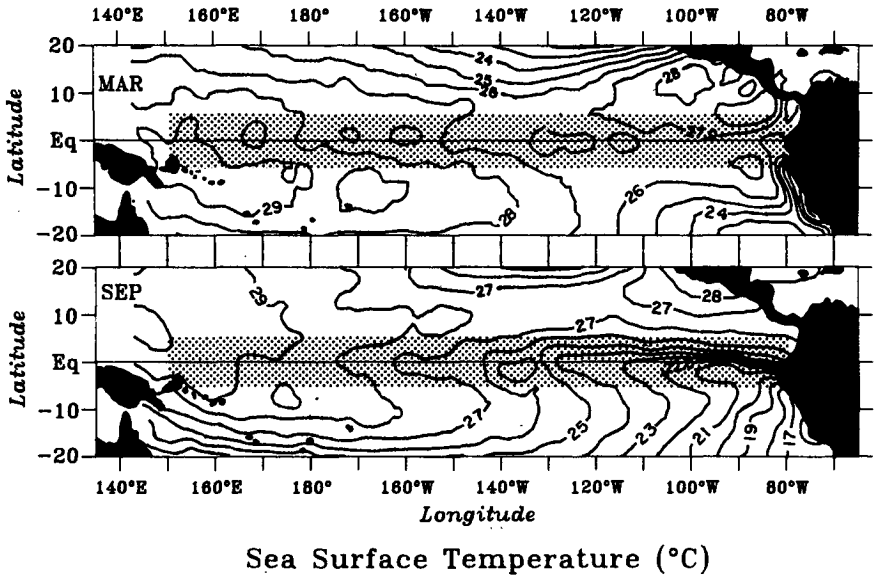

FIG. 1. Climatological distributions of tropical Pacific sea surface temperature for March and September, from the climatology by Reynolds (1982). Shading indicates the equatorial region analyzed in this study.

surface (Wyrtki et al., 1977) and in the eastern Pacific the difference may be as much as 2°–3°C from the surface to 20 m. The resulting overestimate of the box temperature is smallest in the western Pacific where the mixed layer is deep (typically 120 m), and larger in the eastern Pacific where the mixed layer is only as deep as the boxes are thick. However, because the rate of storage is proportional to the *time difference* of temperature, the calculation only implies that any vertical irregularities are time-invariant. This assumption is probably no less accurate than are the SST data per se.

Figure 4 shows the time–longitude behavior of SST and the heat storage rate. The characteristics of the temperature (Fig. 4a) have been well described by Horel (1982) and include three salient features: 1) there is a strong annual cycle in the eastern Pacific with the annual maximum in March–April and the minimum in September–October; 2) the strongest zonal gradient occurs during the Boreal summer between the Galapagos (90°W) and Line Islands (155°W); and 3) there is a westward migration of the seasonal extrema. The

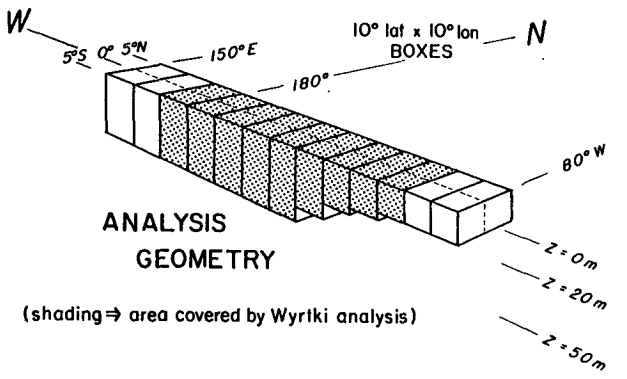

FIG. 2. Perspective sketch of the 10° latitude by 10° longitude boxes used in the analysis. The meridional scale is somewhat exaggerated in comparison with the zonal scale and the vertical scale much more so. The box thickness is reduced from 50 m at 145°W to 20 m at 105°W. Shading on the boxes indicates the 100°W–170°E zone studied by Wyrtki (1981).

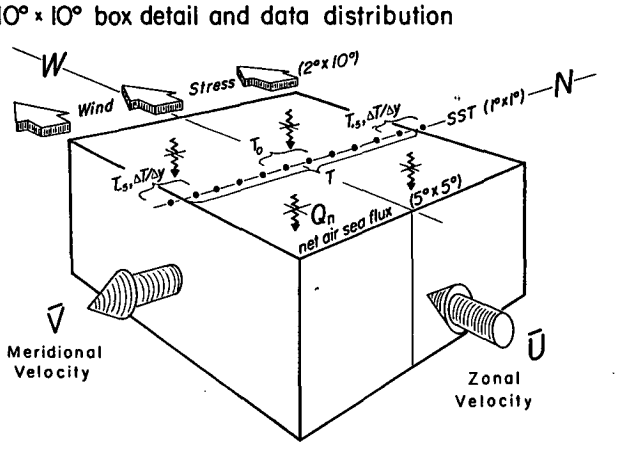

FIG. 3. Perspective sketch showing a single 10° × 10° box and the distribution of gridded climatological data used. Gridded sea surface temperatures are combined to form averages for the whole box, the equator and the meridional flanks (T, T_0 and $T_{\pm 5}$) and temperature gradients at the flanks ($\Delta T/\Delta y$). Four 5° × 5° gridded values of net downward heat flux (Q_n) are combined to obtain the average for the box. Wind stress averages at the equator and the flanks are each obtained by combining two adjacent 2° × 10° grid values to form 4° × 10° values centered at each location.

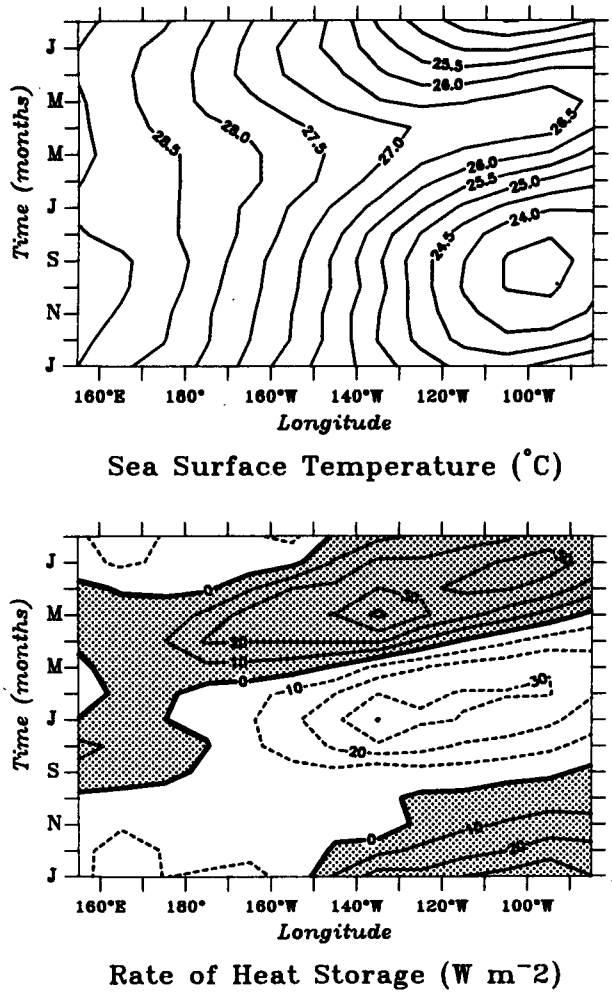

FIG. 4. Time–longitude variations of sea surface temperature (top) and heat storage rate (bottom). In each figure, time advances from December through a complete climatological year (January–December) and ends in January. Longitude advances from the center of the 150°–160°E box (155°E) to the center of the 80°–90°W box (85°W). Positive heating values indicate a gain of heat to the volume and are shaded.

heat storage rate Q_h (Fig. 4b) is only significant in the central and eastern Pacific and consists of alternating periods of warming and cooling that also display a clear westward migration. The heat storage rate and associated annual variation of SST result from seasonal imbalances among the other terms in (1).

5. Net heating and oceanic export

The most straightforward term to deal with in (1) is the net heating (Q_n), since it is given directly by various climatologies. Unfortunately, according to Weare et al. (1981a) it is also a very inaccurate term because it is computed as the difference between large component fluxes of opposite sign (incoming shortwave radiation versus longwave backradiation and latent heat loss) and because those fluxes are based on bulk formulas representing processes for which few reliable estimates exist, and on marine weather observations containing inherent errors and biases. Weare et al. (1981a) estimate the global statistical uncertainty for this term to be 49 W m^{-2} (95% confidence interval). Most of the calibrations of bulk parameters have been made at middle and high latitude locations in the Northern Hemisphere. It is the presumption of their representativeness in other regions plus the assumptions made about data biases that mostly account for the differences between the various climatologies, which are otherwise based on essentially the same data sources.

A number of climatologies have been published that show the surface heating over the equatorial Pacific. Most have used the bulk formula method, e.g., Wyrtki (1965), Weare et al. (1981a,b), Esbensen and Kushnir (1981) and Reed (1985). In addition, there are studies that have calculated the surface flux as a residual loss from the atmosphere after accounting for atmospheric advection and gains and losses at the top of the atmosphere, e.g., Oort and Vonder Haar (1976) and Hastenrath (1980). However, only two of the climatologies are available in a gridded form for each month of the year: Weare et al. (1981b, henceforth WE) and Esbensen and Kushnir (1981, henceforth EK). Though these two climatologies are shown by Talley (1984) to be quite different near 30°N in the Pacific, they are similar along the equator, especially in the central Pacific. In the detailed time–longitude calculations of this study I have used the WE dataset for Q_n. Discussions of the differences between the climatologies are found in Talley (1984), Reed (1985) and elsewhere and will not be considered here. In sections 10 and 12, however, I compare the results of the model using the annual summaries of Q_n from the WE, EK and Reed (1985) climatologies.

There is an inherent overestimate of Q_n involved in the use of surface climatologies: not all of the net downward irradiance is absorbed within the thickness of the boxes. About 5–10% of the total surface irradiance (10–20 W m^{-2}) penetrates below the base of the 20 m thick boxes in the eastern Pacific, based on the optical water types normally found there (Jerlov, 1968). Although the water clarity (transmissivity) increases westward, this loss decreases to less than 3–5% (5–10 W m^{-2}) in the western Pacific due to the greater box thickness used there. No correction has been attempted, however, because such an adjustment would imply an equally accurate knowledge of the component fluxes in Q_n, which we do not have. The net heating in each 10° × 10° box is computed as a simple average of the four corresponding 5° × 5° grid values in the climatology (Fig. 3).

Figure 5a summarizes the time–longitude variations of Q_n, showing a semiannual oscillation in the western and central Pacific, giving way to a predominantly annual cycle in the eastern Pacific. The semiannual vari-

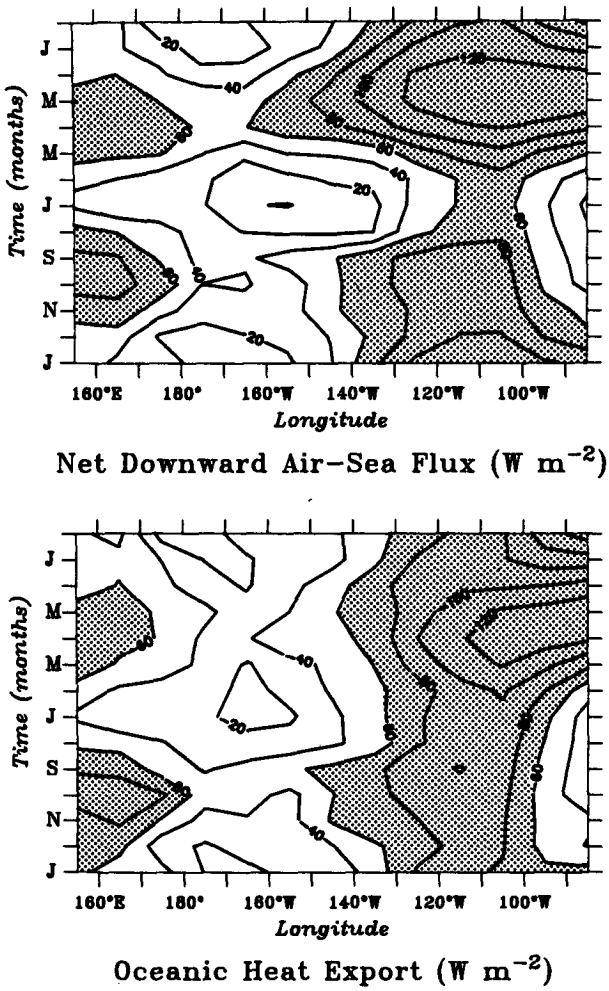

FIG. 5. Time–longitude variations of the net downward air–sea heat flux (top) and the total oceanic heat export (bottom). Magnitudes greater than 60 W m^{-2} are shaded; axes and heat flux signs are as described for Fig. 4.

ation has minima in December–January and June–July and maxima in March–April and August–October. This occurs because the meteorological equator crosses the geographic equator twice yearly, as do the attendant factors that influence the atmospheric heat fluxes. This is not the case in the east, where the southeast trade system dominates. There the first maximum is greatly enhanced, while only a hint of the second (September–October) remains and June–July is the only detectable period of minimum values. The maps of Weare et al. (1981a) show that the larger values of Q_n east of 130°W are primarily due to a smaller total cloud fraction (increased solar radiation) and decreased surface wind speeds and SST (reduced evaporation). These same features are intensified early in the year to produce the strong January–April maximum of Q_n seen in Fig. 5a (see also Reed, 1983).

The heat that must be collectively exported by the advective and diffusive processes within the ocean corresponds to the sum of terms in parentheses in (1) and may be referred to as the total oceanic heat flux divergence, Q_0. It is calculated as the difference between the heat storage rate (Q_h) and the net heating (Q_n). The time–longitude distribution of Q_0 is shown in Fig. 5b. From the similarities between Figs. 5a and 5b it is evident that the oceanic export is closely related to the surface heating. The seasonal variation in the heat storage rate (Fig. 4b) results partly from a phase-shift between Q_n and Q_0 in the eastern Pacific. One can see, for example, that the greatest export occurs in March–April, one month later than the annual heating maximum.

6. Meridional advective heat flux

The contribution of meridional advective fluxes to the heat balance is figured separately for the five degree bands north and south of the equator, then added together. In each case the meridional heat divergence is estimated as

$$Q_v = -(\rho C_p/\Delta x \Delta y) M_{\pm 5}(T_{\pm 5} - T_0 - \Delta T_z), \quad (2)$$

where Δx and Δy are the horizontal dimensions of each box, $M_{\pm 5}$ and $T_{\pm 5}$ are the meridional transport and SST at either flank, T_0 is the SST at the equator and ΔT_z is an estimate for the weak stratification between the surface and the bottom of the box.

The heat flux divergence Q_v and its variations depend strongly on the SST differences between the equator and the north–south flanks of the boxes ($T_{\pm 5} - T_0$). These differences are determined directly from the SST climatology by Reynolds (1982). The greatest contribution comes from the northern flank (Figs. 1, 6a), where the Equatorial Front separates the cool SEC from the warm North Equatorial Countercurrent (NECC). This SST gradient is largest in the central and eastern Pacific, where it is maximum in May–December and smallest in January–April. The gradient south of the equator (Fig. 6b) is only about a degree or less, being largest in the central Pacific.

The calculations are also sensitive to the choice of ΔT_z. This parameter is small in the western Pacific where the mixed layer is considerably deeper than the box thickness of 50 m, and large in the eastern Pacific where the upper portion of the thermocline lies immediately below the boxes. From summaries of hydrographic sections kindly provided by H. L. Bryden, I have calculated average ΔT_z values (5°N–5°S) of 0.3°C for 0–50 m at 150°W and 0.7°C for 0–25 m at 110°W. Cross-equatorial temperature sections by Leetma (1982) confirm the value at 110°W and suggest that 2°C is a reasonable choice at 85°W. As used here the zonally dependent ΔT_z increases linearly from 0.1°C at 155°E to 0.7°C at 105°W and from there to 2.0°C at 85°W.

The meridional transport used in the calculation of Q_v is derived from the 2° latitude by 10° longitude gridded wind stress climatology of Wyrtki and Meyers (1976). The zonal wind stress (τ^x) variations at 5°N and 5°S are shown in Fig. 7. The stress at the north (south) flank is primarily influenced by the NE (SE) trade system and is strongest in December–March (June–October). The annual range at both latitudes is largest in the central and western Pacific, while the greatest annual averages are found in the central Pacific. Both the range and the annual average are greater at the north flank than at the south flank and the annual maxima of the NE and SE systems occur in opposite seasons.

The values of τ^x at 5°N and 5°S are used to compute the poleward Ekman transports (M_e) according to $-\rho f M_e = \tau^x$, where f is the Coriolis parameter at ±5° latitude. Although the meridional transport is dominated by the Ekman effect at most longitudes, it must be adjusted for that portion of the convergent geostrophic flow that occurs within the thickness of the box. (The geostrophic convergence *below* the box provides compensation—through upwelling—for the net divergence within the Ekman layer.) In Wyrtki's (1981) analysis, the geostrophic transports through the meridional flanks of the box are estimated from the zonal differences in observed dynamic heights at the western (170°E) and eastern (100°W) ends. Because hydrographic data cannot provide the zonal and seasonal resolutions required here, it is assumed that the zonal pressure gradient 1) balances the zonal wind stress at the equator and 2) is uniform over the north–south extent of each box. The latter assumption forces the geostrophic transport at the two flanks to be equal, whereas Wyrtki (1981) finds the transport at 5°S to be slightly larger (by 5×10^6 m^3 s^{-1}) than at 5°N. The

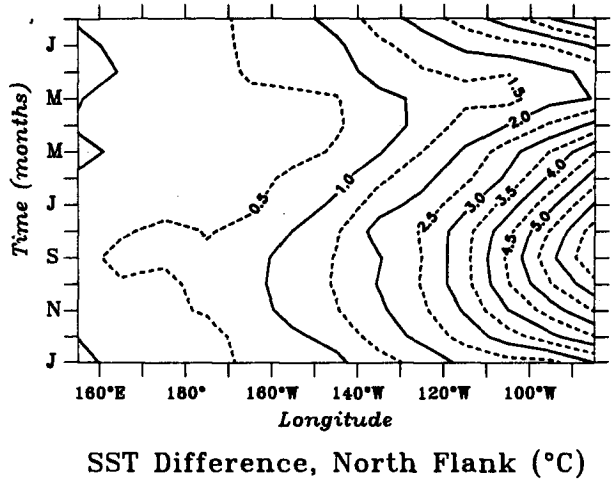

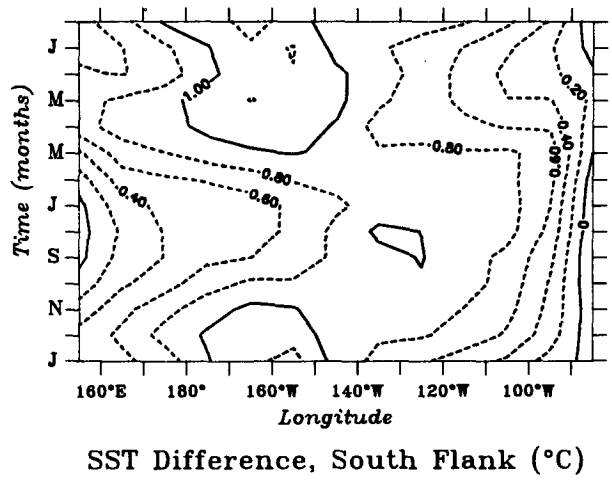

FIG. 6. Time–longitude variations of the difference in sea surface temperature between the north flank of the boxes and the equator (top) and between the south flank and the equator (bottom). Positive values indicate that the equator is colder. Axes are as described for Fig. 4.

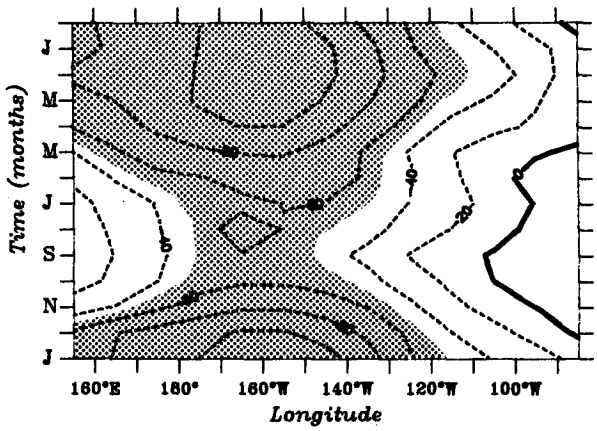

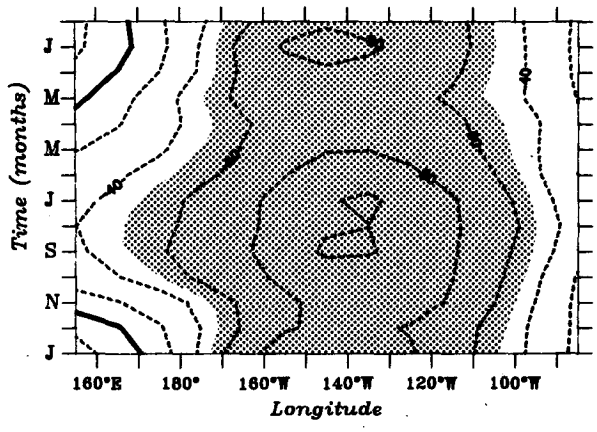

FIG. 7. Time–longitude variations of the zonal wind stress at 5°N (top) and at 5°S (bottom). Negative values indicate westward direction and magnitudes greater than 50 N m^{-2} are shaded. Axes are as described for Fig. 4.

net meridional transport (M^y) across both the north and south flanks of a box is computed as the sum of the two Ekman contributions (±5°) plus twice the geostrophic component: $-\rho f M^y = \tau_{+5}{}^x + \tau_{-5}{}^x - 2 \cdot \gamma(x) \cdot \tau_0{}^x$, where $\gamma(x) = 2 \cdot H(x)/Z_{14} - [H(x)/Z_{14}]^2$ is the fraction of the total geostrophic transport within $H(x)$ of the sea surface and Z_{14} is the depth of the 14°C isotherm as determined by Meyers (1979). This formulation is based upon the assumption that the geostrophic velocity decreases linearly with depth to negligible values at the bottom of the thermocline (near the 14°C isotherm) as suggested by Wyrtki's (1981) analysis.

Table 1 gives a summary of the annual variation of the individual Ekman and geostrophic transport components and the net meridional transport divergence averaged over the 100°W–170°E longitude range. Averaged over the year the southward Ekman component is dominant. This does not necessarily imply a net dominance of transport into the Southern Hemisphere over the long term because the compensating effect of the northward geostrophic transport at 5°S being larger than the southward component at 5°N (found by Wyrtki, 1981) has not been accounted for here and is of the same order as the difference between the Ekman components. Wyrtki's net cross-equatorial geostrophic transport is small, however, and does not affect the strong seasonal shift in the prevailing Ekman transport between the south and north flanks. The Ekman transports go through inverse annual cycles, the northward component dominant from December through April, the southward one from May through November. About two-thirds of the water upwelled at the equator goes into the winter hemisphere.

If we assume that the zonal transport is nondivergent, then the net meridional transport divergence is also the amount of water upwelled. In this way Wyrtki (1981) estimates the annual upwelling to be 50×10^6 m^3 s^{-1} over this region, as compared with 60×10^6 m^3 s^{-1} found in this study (Table 1). This difference is not due to the formulation used here for the geostrophic component, since both it and the Ekman contribution shown in Table 1 are also about 20% higher in magnitude than Wyrtki's estimates. The discrepancy is unaccounted for because the Ekman calculations in both studies are based only on the Wyrtki–Meyers (1976) wind stress climatology. A zonal transport divergence does exist that is accounted for in the calculation of the zonal advection term (next section), but the resulting error in the upwelling estimate is small.

TABLE 1. Annual variation of the meridional transport components and total transport (10^6 m^3 s^{-1}), integrated over the 100°W–170°E longitude zone. Positive (negative) values indicate poleward (equatorward) transport. The total transport is calculated as the sum of the southward and northward components plus twice the geostrophic component (see text).

Month	Southward	Geostrophic	Northward	Total
Jan	53	−22	63	73
Feb	45	−19	67	74
Mar	44	−19	66	71
Apr	46	−17	56	67
May	47	−19	42	51
Jun	55	−22	38	50
Jul	65	−21	34	57
Aug	60	−20	33	54
Sep	67	−19	24	52
Oct	60	−18	28	52
Nov	52	−20	41	54
Dec	45	−19	60	67
Year	53	−20	46	60

As with the volume transport, the flow of heat through upwelling and meridional advection is predominantly into the winter hemisphere. However, the southward heat flux in the Austral winter is much stronger than the northward flux, while in the Boreal winter the northward flux dominates only slightly (not shown). Over the year the southward and northward heat fluxes are about equal west of the Line Islands, but the southward component becomes progressively more dominant east of 150°W. At 100°W more than 80% of the heat is exhausted through the south flank, and east of the Galapagos the heat flux is southward at *both* flanks. These results appear contradictory at first because the differences in the annual volume transport patterns are not large (Table 1) while the SST gradients at the north flank are generally greater than at the south flank (Fig. 6). Both the volume transport and the SST gradients at the southern boundary are relatively uniform in time and space (Figs. 6 and 7). At the north flank, however, they are both highly variable, and the greatest volume transport occurs at times and locations for which the SST gradients are smallest. Hence, the fact that the volume transport and SST gradients combine nonlinearly in (2) gives a very different result here than if these variables are first averaged zonally and/or annually.

The time–longitude variability of the net meridional transport divergence M^y is shown in Figure 8a. The contour labels refer to the divergent flow *per box* at the times and longitudes to which the contours apply. The NE trades with their large seasonal cycle clearly dominate the annual pattern. The SE trades produce a weak secondary maximum in the central Pacific during July–September, but this is not revealed by the contouring. The effect of the semiannual variation of the combined wind systems can be more easily seen in the plot of the heat flux divergence, Q_v (Fig. 8b). Again, however, the annual variation is dominated by the NE trades. The distribution of Q_v more closely resembles the variations of the net poleward transport (Fig. 8a) than those of the meridional SST differences (Fig. 6). The latter express their influence in the eastward displacement of the central Pacific maximum in Q_v relative to that of the transport. The positive values of Q_v in the east during the Boreal summer–fall are due to the occurrence

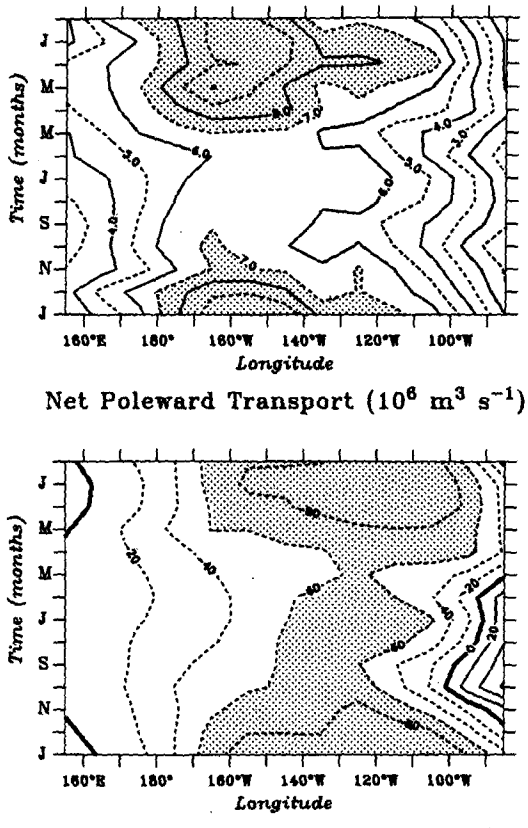

FIG. 8. Time–longitude variations of the net meridional transport through the north and south flanks of the boxes (top) and of the meridional advective heat flux divergence (bottom). Transports are negative, indicating flow away from the equator; axes and heat flux signs are as described for Fig. 4.

of westerly wind stress at 5°N in conjunction with a strong northward temperature gradient (Figs. 6a, 7a).

Averaged over the year and the 100°W–170°E zone the heat removed by meridional advection is 58 W m^{-2}. This is about 25% less than Wyrtki's (1981) calculation, in spite of the fact that the meridional transport calculated here is 20% greater. The reason for this is twofold: 1) Wyrtki assumes an average temperature difference of 4°C between the meridional boundaries and the base of his box, while the same average calculated in this model is 2.65°C; and 2) Wyrtki calculates large scale averages of the input variables prior to their nonlinear combination in (2). In his "likely case" Wyrtki revised his estimate downward to about 65 W m^{-2}, which is closer to the value calculated here.

7. Zonal advective heat flux

The most difficult aspect of the zonal heat flux calculation is our lack of knowledge about the zonal and seasonal variability of the zonal transport. Pilot charts, such as that reproduced by Sverdrup et al. (1942), show westward surface flow across the entire equatorial Pacific. The flow is strongest just west of the Galapagos, where Wyrtki (1965) estimated an average speed of 40 cm s^{-1} between 100°W and 130°W. From there to the dateline the flow is roughly uniform at somewhat smaller values. The zonal component of flow apparently decreases gradually west of the dateline (Sverdrup et al., 1942; Wyrtki, 1981) and from the central Pacific toward South America.

Due to the rapid decrease of westward flow with depth near the equator, the vertically averaged mixed layer flow is generally less than the surface current. Within a degree of the equator in the eastern Pacific the mixed layer transport can actually be eastward due to the strong influence of the upper portion of the EUC (Bryden and Brady, 1985). The best information currently available comes from the Hawaii–Tahiti Shuttle experiment near 150°W (e.g., Firing, 1981; Wyrtki and Kilonsky, 1984) and from the Eastern Pacific Ocean Climate Studies program (EPOCS) near 110°W (e.g., Leetma, 1982; Halpern et al., 1983). From these datasets Bryden and Brady (1985) have constructed composite sections of zonal current at these longitudes from multiyear profiler measurements and geostrophic computations. Using the data kindly provided by H. L. Bryden I have computed the average zonal flow (5°N–5°S) at 150°W and 110°W to be westward at 24 cm s^{-1} (0–50 m) and 20 cm s^{-1} (0–25 m), respectively. For this study I have used the following estimates of the average annual speed of the SEC through the boxes (150°E → 80°W): $U_0(x) = -16, -18, -20, -22, -24, -25, -25, -22, -18, -15, -15, -10$ and -5 cm s^{-1}.

The choice of an annual cycle for the SEC is more difficult. There is probably an equilibrium response to annual and semiannual fluctuations in the trade winds. Part of the transport through the boxes in the central and eastern Pacific is offset by eastward flow in the upper portion of the EUC. The EUC should also have an equilibrium response to the trades. Both the SEC and the EUC would be weaker during periods of weak winds and stronger at other times. Hence, it is not obvious that a strong seasonal variation in the net zonal transport would result.

It is also reasonable to expect that a nonequilibrium response occurs in both currents. Halpern et al. (1983) show that during most years there is a large, impulsive acceleration of flow at 15 m depth revealed by equatorial moorings at 110°W, from weakly westward (about 25 cm s^{-1}) to strongly eastward (50–75 cm s^{-1}). The event has an approximate duration of 3–4 months and reaches its greatest intensity in March, April or May. Much of the variation is due to shoaling and/or intensification of the EUC and is accompanied by a depression of isotherms and a rise in sea level (Halpern et al., 1983; Hayes and Halpern, 1984; Voorhis et al., 1984). The event is apparently caused by an annually occurring equatorial Kelvin wave generated by westerly wind activity in the western equatorial Pacific (e.g., Knox and Halpern, 1982). Unlike the local, equilib-

rium response to wind forcing, this remote response can be expected to weaken the SEC at the same time the EUC is intensified, causing a significant impact on the net transport. However, the annual range in the 5°N–5°S transport must be considerably smaller than suggested by the equatorial measurements, because the amplitude of a first baroclinic mode Kelvin wave would decrease rapidly with meridional distance and would be negligible beyond a few degrees north or south of the equator. Moreover, a climatically averaged event would also have less amplitude because the phenomenon does not occur in the same month each year.

I have estimated the annual variation $\Delta U(x, t)$ of the zonal current based on a least-squares harmonic fit of the mean annual cycle of the Galapagos sea level averaged over the 15 year period from 1960 to 1974. Assuming that this variation decays to negligible amounts at 5°N and 5°S and that the disturbance travels from west to east as an internal Kelvin wave with a first baroclinic mode propagation of $C = 2.7$ m s^{-1}, the resulting model is

$$\Delta U(x, t) = g\{A \cos[\sigma(x/C - t)] + B \sin[\sigma(x/C - t)]\}/f\Delta y, \quad (3)$$

where g is the acceleration due to gravity, σ is the annual frequency, f is the Coriolis parameter at 2.5°N/S, Δy is the meridional distance from 5°S to 5°N and $x = 0$ at the Galapagos. The harmonic constants A and B are −0.56 cm and 2.50 cm, respectively, giving annual ranges of 5 cm in sea level and 15 cm s^{-1} in zonal flow.

The total variation of the zonal flow is $U(x, t) = U_0(x) + \Delta U(x, t)$ and is shown in Fig. 9a. The current reaches maximum values in August–October and is minimum in March–May. The zonal volume transport is obtained by multiplying the current at appropriate longitudes by the cross-sectional areas of the boxes, $M^x(x, t) = U(x, t) \cdot H(x) \cdot \Delta y$. The current and transport are westward (negative) at all times and locations.

The heat divergence due to zonal advective fluxes is calculated as

$$Q_u = (\rho C_p/\Delta x\Delta y)[M_e^x(T_w - T_e)] + \Delta q \quad (4)$$

where the subscripts w, e are used to identify transports or temperatures at the west and east ends of the box, respectively. The temperatures T_w and T_e are taken from the Reynolds SST climatology averaged over the north–south extent of the west and east flanks of each box. The zonal differencing removes most of the vertical inhomogeneities in temperature that may exist within a given box.

The term Δq is a correction applied to account for the divergent part of the zonal flow. Because the transport $M^x(x, t)$ is not zonally uniform there must be an associated transport across the north–south flanks and/or bottom of the box equal to $M_w^x - M_e^x$. In estimating Δq it may be assumed that the amount of water transported out of the box to the west is the sum of that which enters from the east and that which upwells. Any meridional contribution through the north and south flanks of the boxes is presumably geostrophic and has been accounted for in the calculation of the meridional advection term (previous section). The zonal transport divergence is about -1×10^6 m^3 s^{-1} per ten-degree box (downwelling) in the western Pacific and 0.5 to 1.0×10^6 m^3 s^{-1} (upwelling) in the central and eastern Pacific. The rate of heat loss due to zonal transport divergence can be written as

$$\Delta q = (\rho C_p/\Delta x\Delta y)[(M_w^x - M_e^x)(T_w - T_b)], \quad (5)$$

where T_b refers to the temperature at the bottom of a box and is calculated as the north–south average of the SST at the center of the box minus the vertical correction ΔT_z previously used in (2).

The total zonal heat flux divergence resulting from (4) and (5) shows the strongest advective cooling to be in the central Pacific during the Boreal summer when

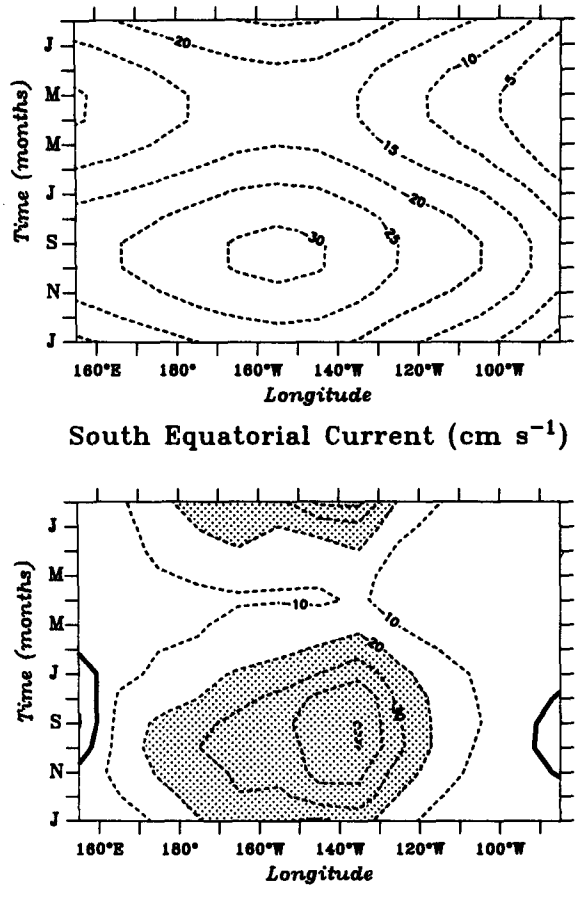

FIG. 9. Time–longitude variations of the average westward flow through the boxes (top) and of the zonal advective heat flux divergence (bottom). Heat flux magnitudes greater than 20 W m^{-2} are shaded; axes and heat flux signs are as described for Fig. 4.

the westward flow and zonal temperature gradient are greatest (Fig. 9b). Very little cooling or warming occurs in the western Pacific, where thermal gradients of any kind are small. East of about 100°W the nondivergent part of the zonal flow [written explicitly in (4)] produces warming due to eastward increases of temperatures off Ecuador. However, the correction for zonal divergence compensates for this such that a weak cooling prevails in the far eastern Pacific.

The annual average of Q_u over the 100°W–170°E zone is -19 W m^{-2}, about one-third of the meridional term, Q_v. Wyrtki (1981) calculated a value of 34 W m^{-2} based on an assumed SEC transport of 15×10^6 m^3 s^{-1}, whereas the average transport here is only 10×10^6 m^3 s^{-1}. The lower transports in this model are partly due to smaller average velocities and partly to the decreased layer depths considered for the eastern sector. For his "likely case" Wyrtki revises his zonal advection estimate downward to a value similar to the one found in this study.

8. Meridional diffusive heat flux

There are reasons to believe that meridional diffusive processes cannot be neglected along the equator. Both the mean and the eddy kinetic energy densities there are comparable to those found in other energetic regions such as the Gulf Stream and the Kuroshio (Wyrtki et al., 1976). Moreover, there are large meridional gradients of SST at the north and south flanks of the cold tongue that extends westward from the Galapagos almost to the dateline. The gradient at the north flank is especially strong during the Boreal summer months, when it is seen to coincide with cusp-shaped, westward-propagating patterns in SST (Legeckis et al., 1983). Work by Philander (1976, 1978) and Cox (1980) seems to establish that these waves and their associated eddy motions result from a barotropic instability created by the meridional shear between strong zonal currents.

In a recent analysis of drifter motions between 100° and 140°W, Hansen and Paul (1984) directly compute the meridional eddy heat flux associated with the wave motions during June–October 1979. They estimate a total gain between 5°N and 5°S of about $Q_{d,y} = +45$ W m^{-2}, yielding a meridional eddy diffusivity of $K_y = 4 \times 10^4$ m^2 s^{-1}, more than an order of magnitude larger than that assumed by Wyrtki (1981). The results of Cox's (1980) model suggest that the thermal diffusivity was probably maximum over the area and period covered by the drifter study because K_y depends on the availability of eddy kinetic energy (meridional shear of zonal flows). Cox's model shows maximum eddy kinetic energy density from the Galapagos Islands westward to the dateline, decaying to small values elsewhere. The period studied by Hansen and Paul also coincides with the time of year in which the SST manifestations of the eddies are most detectable (Legeckis et al., 1983). Hence, this value of K_y may be an upper limit.

The pointwise meridional diffusive flux density is proportional to K_y times the second derivative of the temperature distribution in the north–south direction. Assuming K_y to be meridionally invariant the integrated heat flux divergence (in terms of an equivalent surface flux) is given by

$$Q_{d,y} = \rho C_p K_y H(x) \cdot [\Delta T_{+5}/\Delta y - \Delta T_{-5}/\Delta y]/\Delta y, \quad (6)$$

where $\Delta T_{+5}/\Delta y$ and $\Delta T_{-5}/\Delta y$ are the meridional temperature gradients at the north and south boundaries. The gradients are well resolved by the Reynolds SST climatology and their magnitudes are additive for most longitudes because they are oppositely directed on either side of the equator. As a test of (6), $Q_{d,y}$ was first averaged over the Hansen-Paul space–time domain using their value of K_y, and a heat flux divergence of +47 W m^{-2} was recovered. The close approximation to their estimate is not surprising because their value of K_y was determined using the reverse calculation and similar climatological temperature gradients.

The choice of K_y is difficult because virtually nothing is known of its spatial and temporal variations, though such variations must surely be significant. Assuming that the Hansen–Paul value (4×10^4 m^2 s^{-1}) is an upper bound, I have assigned a value $K_y = 2 \times 10^4$ m^2 s^{-1} for all longitudes and months of the year. The meridional diffusion of heat into the equatorial zone given by (6) is shown in Fig. 10. It is strongest from 120° to 160°W, fading to negligible or slightly negative values near the Galapagos and west of the dateline. Since the only variable input apart from temperature is the zonally dependent box thickness, the pattern of variation is almost identical to that of the difference between the northern and southern temperature gradients in (6) (not shown).

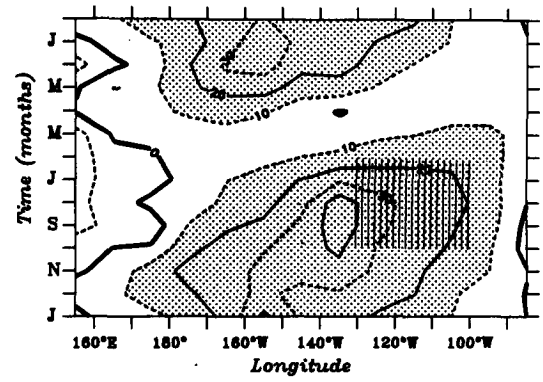

FIG. 10. Time–longitude variations of the meridional diffusive heat flux divergence. Light shading indicates heat gain in excess of 10 W m^{-2} and the shaded square indicates the time–longitude domain for which Hansen and Paul (1984) estimated this term directly from perturbation data. Axes and heat flux signs are as described for Fig. 4.

Because the SST gradients are more intense north of the equator, $Q_{d,y}$ is much larger at the north flank than at the south flank, the difference becoming greater toward the east. Combining this with the advective transport patterns discussed in section 6, there is a total cross-equatorial (nondivergent) heat flux from the Northern into the Southern Hemisphere over the year. This is quite the opposite to what one would intuitively expect based only on long-term averages of wind stress and SST. This result highlights the importance of 1) accounting for seasonal and zonal variations in the meridional advection and 2) including the effects of meridional diffusion.

9. Uncertainties

It is important to quantify in some way the uncertainties in the terms before attempting to discuss the balance. In the remaining discussions, in which large-scale zonal and temporal averages are used, systematic errors in the empirical parameters and unknown biases in the data inputs are assumed to be the only significant sources of uncertainty. The effects of random errors are mainly important when examining smaller time and space scale features, where fewer individual observations are incorporated into the averages.

In the calculation of the oceanic flux divergences discussed above (Q_u, Q_v, $Q_{d,y}$), the data inputs are sea surface temperature (SST), estimated average zonal transport in the mixed layer (U_0), mixed layer stratification (ΔT_z) and zonal wind stress (τ^x). The only empirical parameter involved is the meridional thermal diffusivity (K_y). The effects of SST can be ignored because only the zonal and meridional differencing of SST is involved, which eliminates biases in that variable. One can place ad hoc limits on the errors in the remaining parameters but it is not obvious how they translate into an overall uncertainty for the combined oceanic fluxes after such limits are exercised through the defining equations (2)–(6).

To estimate the combined uncertainties in the total advective flux divergence $Q_u + Q_v$ due to systematic errors in the inputs, the calculations in (2)–(5) were repeated for all possible combinations in which the uncertain inputs were separately assigned either (i) their optimally estimated values as discussed in previous sections, or (ii) their minimum or maximum values above or below the optimal values. For each combination of perturbed inputs the heat flux terms were calculated and added and the average and standard deviations computed for all combinations. The minimum and maximum values of U_0 and ΔT_z were set at 50% above or below the optimal estimates. Wind stress was set either at the Wyrtki-Meyers values, as a minimum, or at 20% above those values, as a maximum. This is based on Bryden and Brady's (1985) finding that stresses in the newer Hellerman and Rosenstein (1983) climatology run about 20% above the Wyrtki–Meyers values. No "optimal" values were assigned to stress as there is no a priori basis at present for choosing between the two climatologies.

The above choices give rise to $3 \times 3 \times 2 = 18$ combinations. The means and standard deviations for $Q_u + Q_y$ are -28 ± 7, -99 ± 17, and -52 ± 17 W m^{-2} for the western, central and eastern Pacific, respectively. While a ± 15–20 W m^{-2} uncertainty may seem reasonable, it seems anachronous that the western Pacific (for which we have few oceanic observations) should have the smallest uncertainty. This occurs because all of the flux calculations depend on zonal, meridional and vertical temperature differences, which are much smaller in the western Pacific. Expressed as percentages of the mean values the estimated rms errors are $\pm 25\%$, $\pm 17\%$ and $\pm 33\%$, respectively, which qualitatively agree with our relative knowledge of the three areas.

This kind of analysis can be extended to include the meridional diffusion term by assigning ad hoc, order of magnitude limits on K_y of 10^4 and 10^5 m^2 s^{-1}. This increases the number of combinations to 36 and the estimated rms errors for $Q_u + Q_v + Q_{d,y}$ are ± 20, ± 54 and ± 33 W m^{-2} respectively for the western, central and eastern Pacific. Thus, the assignment of order of magnitude limits to K_y increases the overall uncertainty considerably beyond that associated with the advective fluxes alone.

10. Residual heat flux divergence

Tables 2 and 3 give spatially and temporally averaged summaries of the calculations discussed in sections 5–8. The results are obtained using the WE climatology for Q_n. Table 2 lists the annual means of all terms except Q_h (which averages to zero) for each $10° \times 10°$ box, with a zonally integrated summary for the 100°W–170°E zone studied by Wyrtki (1981). Table 3 presents zonal (100°W–170°E) averages of the various terms for individual months of the year. Averaged over the year, all of the directly computed flux divergences (Q_u, Q_v, and $Q_{d,y}$) are largest in the central Pacific where the equatorial easterly winds are best developed, zonal transport is maximum and horizontal SST gradients are greatest (Table 2). Zonal averages of these terms are also greatest during that time of year (August–February) when the combined trades are strongest and the equatorial cold tongue best developed (Table 3). Annual averaging gives overall estimates of -24, -70 and -37 W m^{-2} respectively for $Q_u + Q_v + Q_{d,y}$ in the western, central and eastern Pacific. The corresponding annual averages of the advective terms alone ($Q_u + Q_v$) are -27, -91 and -48 W m^{-2}.

The residual heat flux divergence is calculated as $Q_\Delta = Q_h - Q_n - Q_u - Q_v - Q_{d,y}$. The fact that spatial and temporal averaging leads to a zero residual (right bottom corner in Tables 2 and 3) gives the illusory impression that a reasonable balance has been achieved. The zonal and seasonal distributions of Q_Δ tell us otherwise.

TABLE 2. Annual mean values of heat flux divergence due to net air-sea exchange (Q_n), zonal advection (Q_u), meridional advection (Q_v), and meridional diffusion ($Q_{d,y}$). The net downward heat flux at the sea surface (Q_n) is from the climatology by Weare et al. (1981a,b). The residual oceanic flux (Q_Δ) is calculated as $Q_\Delta = -Q_n - Q_u - Q_v - Q_{d,y}$. Means are given for 10° × 10° areas centered at ten degree longitude intervals from 155°E to 85°W (left to right). On the far right is the mean for the 100°W–170°E longitude zone studied by Wyrtki (1981). Vertical lines separate longitude zones that have been used to define the western, central and eastern Pacific in the text.

	Longitude (deg)													
Term	155	165	175E	175W	165	155	145	135	125	115	105	95	85	100W–170E
Q_n	64	65	48	30	25	34	49	61	88	97	105	78	64	60
Q_u	0	−11	−14	−19	−25	−19	−28	−41	−14	−9	−5	−5	−3	−19
Q_v	0	−11	−19	−33	−53	−60	−68	−65	−86	−68	−68	−37	7	−58
$Q_{d,y}$	−8	3	3	14	18	24	20	29	20	17	14	10	1	18
Q_Δ	−56	−46	−18	8	35	21	27	16	−8	−37	−46	−46	−69	+0

If there were no net errors after the summation of terms in Q_Δ, then by (1) this residual would be negative everywhere, corresponding to a diffusive heat loss $Q_{d,z}$ across the bottom of the boxes. It is not. The annual mean residuals averaged over the western, central and eastern Pacific zones are −28, +20 and −50 W m^{-2}, respectively. The null average for 100°W–170°E turns out to be the fortuitous result of combining the positive values in the central Pacific with negative values to the east (Table 2).

Figure 11 graphically summarizes the results for Q_Δ given in Tables 2 and 3. Because the vertical diffusive flux through the bottom of the boxes cannot be positive, there must be a net negative error among the terms Q_n, Q_u, Q_v and $Q_{d,y}$ in the central Pacific, to account for the positive residual values there. For many of the individual months of the year and 10 degree longitude zones the residual flux reaches values as high as +50 to +80 W m^{-2} (this is not evident in Fig. 11 due to the smoothing used in the contouring program). The largest values of Q_Δ occur sporadically, however, and reflect noisiness in the climatologies for the net heating, Q_n. Annual averages as high as +27 and +35 W m^{-2} occur for individual boxes (145°W, 165°W), and zonal averages (100°W–170°E) as high as +31 and +24 W m^{-2} for individual months (December–January). It is more likely that these larger scale averages result from systematic errors in one or more of the estimated terms of the balance. To explore further the imbalance we must try to understand what the residual heat flux should simulate.

11. Vertical diffusion

The vertical diffusive flux $Q_{d,z}$ must be always and everywhere negative, corresponding to an export of heat from the warmer upper layer to the colder water below. We expect vertical diffusion to be most important in the upper portion of the EUC where a strong shear exists between the EUC and the overlying SEC, in conjunction with a vertical gradient of temperature (the upper portion of the thermocline) and the availability of kinetic energy from wind mixing. Unfortunately, little is directly known about the zonal and meridional

TABLE 3. Annual variation of the terms in the equatorial heat balance, averaged over the 100°W–170°E longitude zone. The net downward heat flux (Q_n) is from the climatology by Weare et al. (1981a,b).

	Heat flux divergence (W m^{-2})						
Month	Q_h	Q_n	Q_0	Q_u	Q_v	$Q_{d,y}$	Q_Δ
Jan	9	57	−48	−16	−76	21	24
Feb	20	79	−59	−12	−77	20	9
Mar	28	97	−69	−8	−61	14	−14
Apr	15	91	−76	−6	−53	5	−22
May	−8	57	−64	−9	−42	6	−19
Jun	−20	29	−49	−14	−46	9	2
Jul	−23	24	−47	−21	−55	16	13
Aug	−14	35	−49	−28	−59	24	14
Sep	−3	71	−73	−33	−40	22	−22
Oct	−3	68	−71	−32	−49	25	−15
Nov	−3	60	−63	−28	−62	28	−2
Dec	2	47	−45	−25	−75	22	31
Year	0	+59	−59	−19	−58	+18	0

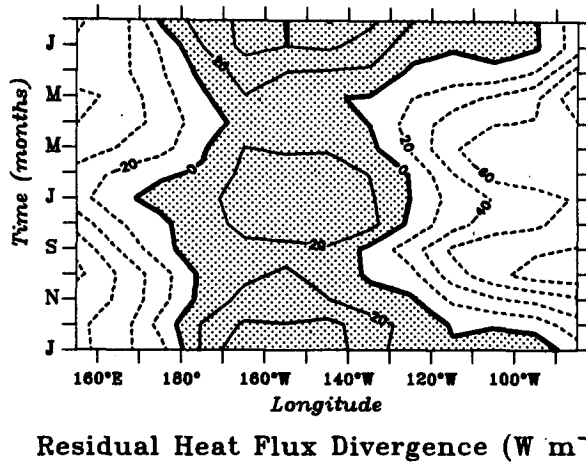

FIG. 11. Time–longitude variations of the residual heat flux divergence, as defined in the text. Positive values are shaded; axes and heat flux signs are as described for Fig. 4.

distribution of $Q_{d,z}$. A downward diffusive heat loss of about -20 W m^{-2} has been estimated from microstructure measurements at 150°W near the equator, yielding vertical diffusivities (K_z) of up to 10^{-3} m^2 s^{-1}, roughly uniform from 20 m depth to the upper portion of the thermocline (Crawford, 1982). Similar measurements above the EUC in the Atlantic suggest the range $10^{-4} < K_z < 10^{-3}$ m^2 s^{-1} (Osborn, 1980) and recent work by Gregg et al. (1985) gives the same range at 140°W in the Pacific. Preliminary results from another recent section of microscale measurements along 140°W from 3°S to 3°N indicate that the mechanical dissipation rate is independent of latitude within the sampling domain, rather than decreasing away from the equator and the EUC as previously supposed (Moum et al., 1986).

Composite temperature sections from the Hawaii–Tahiti Shuttle and the EPOCS experiments give vertical temperature gradients of 0.1°C/10 m at 50 m depth and 0.6°C/10 m at 25 m, computed as averages from 5°S to 5°N along 150°W and 110°W, respectively. If a zonally and meridionally uniform diffusivity of $10^{-4} < K_z < 10^{-3}$ m^2 s^{-1} is assumed, we get -4 to -40 W m^{-2} of cooling near the Line Islands and -25 to -250 W m^{-2} west of the Galapagos. It probably makes more sense, however, to assume that the mechanical dissipation (rather than K_z) is spatially uniform. In that case a range for $Q_{d,z}$ of -5 to -50 W m^{-2} would be consistent with existing microscale measurements. Until future turbulence measurements give us more information about the zonal and meridional distribution of K_z, the uncertainties about the diffusive contribution remain large and there seems to be no a priori basis for postulating any particular zonal distribution of vertical diffusive heat flux. As a reference for the following discussion I shall assume that vertical turbulence removes at least 10–40 W m^{-2} from the surface layer, taken as a zonal and annual average over the cold tongue.

12. Discussion

Upwelling due to poleward Ekman transports constitutes the dominant advective process, removing about 60 W m^{-2} of heat from the equatorial zone (100°W–170°E) as opposed to 20 W m^{-2} for zonal advection by the SEC. Conclusions about the remainder of the balance are conditioned by one's choice of a climatology for the net heat gain from the atmosphere (Q_n). The advective transports remove more heat than is gained across the sea surface according to the WE and EK climatologies (e.g., Table 2). For the central Pacific alone (120°–170°W) the difference is 41 W m^{-2}, an amount that exceeds the rms error limits estimated for the advective terms severalfold. If an additional 20 W m^{-2} are removed by vertical diffusion, the total deficit in the central Pacific rises to about 60 W m^{-2}. Using the Reed climatology for Q_n the advective terms remove 80% of the surface heat gain in the central Pacific, leaving 20 W m^{-2} to be removed by vertical diffusion. However, about 70 W m^{-2} must be removed in the western and eastern Pacific. Hence, if the WE and EK climatologies are correct, there must be a large heat gain in the central Pacific due to meridional diffusion, the only remaining oceanic term. If the Reed climatology is correct the meridional diffusion is not necessary, but without it one must explain why the negative residuals have such large magnitudes in the east and west.

With the oceanic flux divergences Q_u, Q_v and $Q_{d,y}$ calculated from the optimal inputs discussed in sections 6–8, Fig. 12 compares the zonal distributions of residuals that result from using the net downward flux from the WE, EK and the Reed (1985) climatologies. The WE values have already been used in Tables 2 and 3. When these distributions are compared with the postulated minimum cooling rates from vertical diffusion (shading), the most reasonable fits are given by Weare et al. in the west, Reed in the central Pacific and Es-

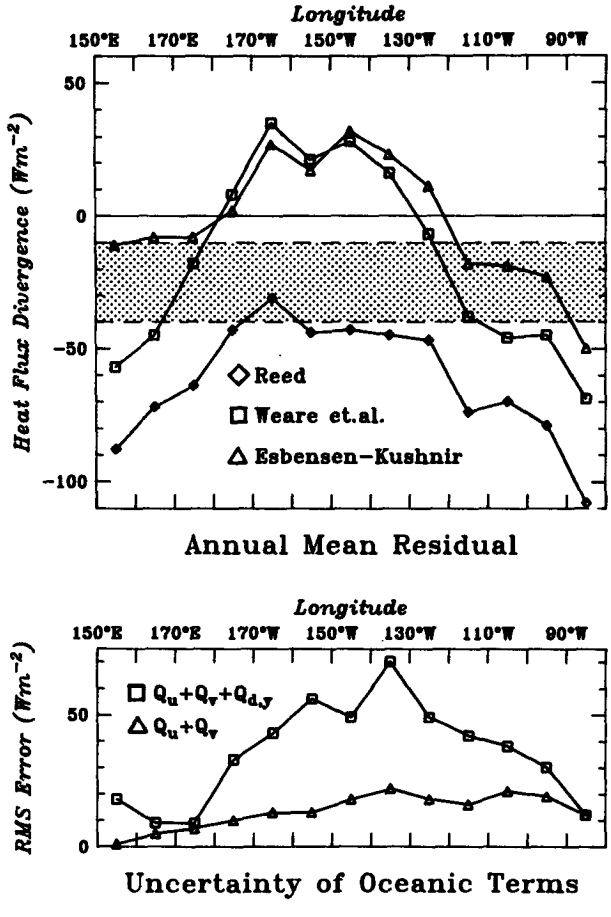

FIG. 12. Top: annual mean residual heat flux across the equatorial Pacific using three different climatologies for the net downward heat flux. The ad hoc estimated range for the minimum heat removed by vertical turbulence is indicated by shading. Bottom: the estimated rms errors of calculated oceanic heat flux divergences.

bensen and Kushnir in the east. The most glaring discrepancies are found for three cases: the positive values computed for the central Pacific using the data by 1) Weare et al. and 2) Esbensen and Kushnir, and 3) the large negative values computed for the western and eastern Pacific using the Reed climatology. These features are due to two facets of the balance. The first is that all of the climatologies for Q_n lead to residual fluxes that are considerably more positive (less negative) in the central Pacific than in the western and eastern regions, the contrasts being about 30–50 W m^{-2}. The second is the zonally uniform difference between the Reed climatology and the other two, about 50–60 W m^{-2}.

The least likely explanation for the zonal nonuniformity of Q_Δ is that the process of vertical diffusion behaves in a similar manner. The greatest amount of cooling due to vertical turbulence should take place in the central Pacific where the available kinetic energy from the wind and vertical current shears is strongest and occurs in conjunction with large vertical temperature gradients. Moreover, we qualitatively expect the downward diffusion of heat at the base of the mixed layer to approximately balance the upward advective flux there due to upwelling (taken as a long term average). Since the distribution of zonal wind stress dictates maximum equatorial upwelling in the central Pacific, we also expect the heat removed by vertical turbulence to be greatest there. These expectations run contrary to the zonal character of the residuals in Fig. 12. Finally, it is clear that vertical diffusion cannot *add* heat to the surface layer, as suggested by the residuals using the WE and EK climatologies.

Almost as improbable is the notion that the zonal variation in Q_Δ can be explained by systematic errors in the advection, $Q_u + Q_v$. In the central Pacific, for example, the differences between the postulated range for $Q_{d,z}$ and the value modeled by Q_Δ (using Q_n from WE and EK) are considerably larger than the uncertainty limits estimated in section 9. Moreover, such an explanation would require reducing the advective heat loss by a factor of two in the central Pacific, or greatly increasing advection to the east and west. Either of these adjustments would imply a nearly uniform distribution of advective cooling that is qualitatively inconsistent with the maximum wind stress and transports that are found in the central Pacific.

There are large differences between the three Q_n climatologies, so one or more of them are incorrect, at least by a constant factor. One might argue that the positive residual flux in the central Pacific is due to an underestimation of Q_n by Weare et al. and Esbensen and Kushnir. For all three climatologies the zonal variation of Q_Δ can be eliminated by increasing Q_n by 50–60 W m^{-2} in the central Pacific. It is difficult, however, to imagine systematic errors in bulk parameters that would lead to such an adjustment in one region and not the others.

Barring what seems like an unlikely, strong zonal variation of systematic errors in all three climatologies for Q_n, only the meridional diffusion term $Q_{d,y}$ can explain the zonal distributions of Q_Δ. Larger values of K_y in the central Pacific would reduce or eliminate the zonal nonuniformity of Q_Δ and would at the same time be consistent with the greater availability of eddy kinetic energy expected there due to horizontal current shears, as demonstrated by Cox's (1980) model. Note that the same result cannot be achieved by reducing $Q_{d,y}$ in the western and eastern Pacific because this term is already small in those areas (Table 3).

Neglect of the meridional diffusion increases the positive residuals in the central Pacific to 40–50 W m^{-2} for the Weare et al. and Esbensen–Kushnir climatologies, and the zonal contrasts of Q_Δ increase to 50–60 W m^{-2}. The residuals remain negative for the Reed climatology without meridional diffusion, but the zonal variation also intensifies. In contrast, an increase of the meridional diffusivity K_y by a factor of three to about 6×10^4 W m^{-2} between 120°W and the dateline eliminates zonal variation in the residual flux and makes it negative everywhere for all of the Q_n climatologies. With this modification the WE and EK values for Q_n yield residuals that lie more or less uniformly within the minimum range postulated for $Q_{d,z}$, while Reed's values put Q_Δ in the range −60 to −90 W m^{-2}. Although the latter values are larger than current estimates from turbulence measurements, our present knowledge of the vertical dissipation is probably not adequate to say this is unrealistic.

13. Summary

Seasonal variations in wind stress, currents and temperature gradients result in oceanic heat flux divergences that are greatest from August through February. Zonal advection, meridional advection and meridional diffusion are strongest in the Boreal fall, winter and fall–winter seasons, respectively. The only quantitative conclusion about relative magnitudes is that the heat removed through upwelling and meridional advection is about a factor of three larger than from zonal advection. The relative contributions of the other terms require more investigation.

About two-thirds of the water upwelled in the equatorial zone is advected meridionally into the winter hemisphere. Over the year, the net meridional transports of water through the north and south flanks are about equal. However, the zonal and seasonal resolution of the model plus the inclusion of meridional diffusion yields a strong cross-equatorial heat transport from the Northern to the Southern Hemisphere in the central and eastern Pacific that is not expected solely through a consideration of large scale, long term wind stress and SST patterns.

To summarize the results it is useful to propose an idealization of the heat balance, or what may be called

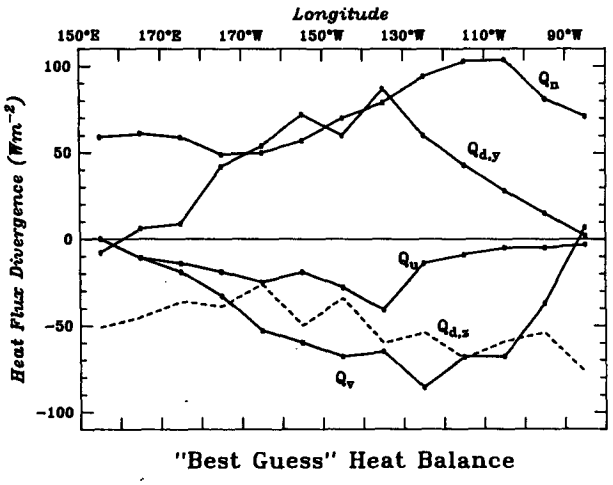

FIG. 13. A postulated heat balance based on an average of three climatologies of net downward heat flux (Q_n) and on modeled oceanic heat fluxes as described in the text. The vertical diffusive heat loss ($Q_{d,z}$) is calculated as the residual (dashed).

a "best guess." Because we know only that the vertical diffusive flux is negative, but not how large, there is no objective basis for determining which of the three climatologies for Q_n is/are biased. Hence, the three climatologies have simply been averaged together. As the most physically consistent means of eliminating the unlikely large zonal variation in the residuals the meridional diffusivity has been set at 6×10^4 m^2 s^{-1} from 120°W to 170°E and decreased linearly to 2×10^4 m^2 s^{-1} from there to 150°E and 80°W. The resulting average for 100°–140°W agrees approximately with Hansen and Paul (1984). The advective terms are kept at their optimal settings as discussed in sections 6 and 7. The zonal distributions of annual mean values are shown in Fig. 13, with the residuals shown as a dashed curve ($Q_{d,z}$).

Based on this analysis, all or most of the possible contributions to the equatorial heat balance appear to be significant, except in the far western Pacific and between the Galapagos and South America. In the central Pacific, where the cold tongue is best developed, comparable amounts of heat are imported from the atmosphere and through meridional diffusion, and the heat is removed by zonal and meridional advection and vertical diffusion. In the western Pacific the balance is primarily between the surface heat gain and vertical diffusion, while in the eastern Pacific (west of the Galapagos) the surface heat gain is mainly offset by meridional advection and vertical diffusion.

The proposed balance may be considered as a "strawman" reference for further research. It is clear that if we are to resolve the questions raised by this analysis we must obtain more measurements of both the meridional and the vertical diffusive fluxes, and that experiments should be planned for at least three widely separated locations in the western, central and eastern longitude zones. Experiments should be conducted during similar seasons, preferably the latter part of the calendar year when the heat fluxes are best developed. The other promising area of research is in the development of newer satellite-based methods for estimating the radiative and evaporative fluxes across the sea surface, as an independent means of assessing the conflicting results from the bulk climatologies.

Acknowledgments. I wish to thank Drs. J. Moum, T. Strub, B. Weare, S. Esbensen, K. Wyrtki, R. Reed, H. Bryden, J. Richman, L. Talley and R. Reynolds for the helpful discussions that have contributed to various aspects of this work. I also wish to acknowledge the NOAA Climate Analysis Center (Dr. R. Reynolds), the University of California, Davis (Dr. B. Weare) and the University of Hawaii (Dr. K. Wyrtki) for providing the gridded climatological data for sea surface temperature, surface heat fluxes and wind stress, respectively. The research has been sponsored jointly by NSF Grants ATM 81-20141 and OCE 84-83790 and by NOAA Grants NA-84RA-D-05043 and NA-85AA-D-CA024.

REFERENCES

Bryden, H. L., and E. C. Brady, 1985: Diagnostic model of the three dimensional circulation in the upper equatorial Pacific Ocean. *J. Phys. Oceanogr.*, **15,** 1255–1273.

Cane, M. A., 1983: Oceanographic events during El Niño. *Science,* **222,** 1189–1194.

Cox, M. D., 1980: Generation and propagation of 30-day waves in a numerical model of the Pacific. *J. Phys. Oceanogr.*, **10,** 1168–1186.

Crawford, W. R., 1982: Pacific equatorial turbulence. *J. Phys. Oceanogr.*, **12,** 1137–1149.

Esbensen, S. K., and V. Kushnir, 1981: *The Heat Budget of the Global Ocean: An Atlas Based on Estimates from Marine Surface Observations.* Climatic Research Institute, Rep. No. 29. Oregon State University, Corvallis, 27 pp., 188 figs.

Firing, E., 1981: Current profiling in the NORPAX Tahiti Shuttle. *Trop. Ocean-Atmos. Newslett.* **5,** 1–9.

Gregg, M. C., H. Peters, J. C. Wesson, N. S. Oakey and T. J. Shay, 1985: Intensive measurements of turbulence and shear in the Equatorial Undercurrent. *Nature,* **113,** 140–144.

Halpern, D., S. P. Hayes, A. Leetma, D. V. Hansen and S. G. H. Philander, 1983: Oceanographic Observations of the 1982 warming of the tropical eastern Pacific. *Science,* **221,** 1173–1174.

Hansen, D. V., and C. A. Paul, 1984: Genesis and effects of long waves in the equatorial Pacific. *J. Geophys. Res.*, **89,** 10 431–10 440.

Harrison, D. E., and P. S. Schopf, 1984: Kelvin-wave-induced anomalous advection and the onset of surface warming in El Niño events. *J. Phys. Oceanogr.*, **14,** 923–933.

Hastenrath, S., 1980: Heat budget of the tropical ocean and atmosphere. *J. Phys. Oceanogr.*, **10,** 159–170.

Hayes, S. P., and D. Halpern, 1984: Correlation of current and sea level in the eastern equatorial Pacific. *J. Phys. Oceanogr.*, **14,** 811–824.

Hellerman, S., and M. Rosenstein, 1983: Normal monthly wind stress over the world ocean with error estimates. *J. Phys. Oceanogr.*, **13,** 1093–1104.

Horel, J. D., 1982: On the annual cycle of the tropical Pacific atmosphere and ocean. *Mon. Wea. Rev.*, **110,** 1863–1878.

Jerlov, N. G., 1968: *Optical Oceanography. Elsevier Oceanography Series,* Vol. 5, Elsevier, 194 pp.

Knox, R. A., and D. Halpern, 1982: Long range Kelvin wave prop-

agation of transport variations in Pacific Ocean equatorial currents. *J. Mar. Res.*, **40**(Suppl.), 329–339.

Leetma, A., 1982: Observations of near-equatorial flows in the eastern Pacific. *J. Mar. Res.*, **40**(Suppl.), 357–370.

Legeckis, R., W. Pichel and G. Nesterczuk, 1983: Equatorial long waves in geostationary satellite observations and in a multichannel sea surface temperature analysis. *Bull. Amer. Meteor. Soc.*, **64**, 133–139.

Levitus, S., 1984: Annual cycle of temperature and heat storage in the world ocean. *J. Phys. Oceanogr.*, **14**, 727–746.

Meyers, G., 1979: Annual variation in the slope of the 14°C isotherm along the equator in the Pacific Ocean. *J. Phys. Oceanogr.*, **9**, 885–891.

Moum, J. N., D. R. Caldwell, C. A. Paulson, T. K. Chereskin and L. A. Regier, 1986: Does ocean turbulence peak at the equator? *J. Phys. Oceanogr.* (in press).

Niiler, P., and J. Stevenson, 1982: The heat budget of tropical warm-water pools. *J. Mar. Res.*, **40**(Suppl.), 465–480.

Oort, A. H., and T. H. Vonder Haar, 1976: On the observed annual cycle in the ocean–atmosphere heat balance over the Northern Hemisphere. *J. Phys. Oceanogr.*, **6**, 781–800.

Osborn, T. R., 1980: Estimates of the local rate of change of vertical diffusion from dissipation measurements. *J. Phys. Oceanogr.*, **10**, 83–89.

Philander, S. G. H., 1976: Instabilities of zonal equatorial currents. *J. Geophys. Res.*, **81**, 3725–3735.

——, 1978: Instabilities of zonal equatorial currents, 2. *J. Geophys. Res.*, **83**, 3679–3682.

Rasmusson, E., and J. M. Wallace, 1983: Meteorological aspects of the El Niño-Southern Oscillation. *Science*, **222**, 1195–1202.

Reed, R. K., 1983: Heat fluxes over the eastern tropical Pacific and aspects of the 1972 El Niño. *J. Geophys. Res.*, **88**, 9627–9638.

——, 1985: An estimate of the climatological heat fluxes over the tropical Pacific Ocean. *J. Climate and Appl. Meteor.*, **24**, 833–840.

Reynolds, R. W., 1982: A monthly averaged climatology of sea surface temperature. NOAA Tech. Rep. NWS-31, 35 pp.

Sverdrup, H. U., M. W. Johnson and R. H. Fleming, 1942: *The Oceans.* Prentice-Hall, 1087 pp.

Talley, L. D., 1984: Meridional heat transport in the Pacific Ocean. *J. Phys. Oceanogr.*, **14**, 231–241.

Voorhis, A., J. R. Luyten, G. Needell and J. Thomson, 1984: Wind-forced variability of upper ocean dynamics in the central equatorial Pacific during PEQUOD. *J. Phys. Oceanogr.*, **14**, 615–622.

Weare, B. C., P. T. Strub and M. D. Samuel, 1981a: Annual mean surface heat fluxes in the tropical Pacific Ocean. *J. Phys. Oceanogr.*, **11**, 705–717.

——, —— and ——, 1981b: *Marine Climate Atlas of the Tropical Pacific Ocean.* Contrib. Atmos. Sci. No. 20, Dept. of Land, Air and Water Resources, University of California, Davis, 147 pp, 254 Figs.

Webster, F., 1984: Ocean Climate Research. *Eos, Trans. Amer. Geophys. Union*, **65**(32), 466–468.

Wyrtki, K., 1965: The average annual heat balance of the North Pacific Ocean and its relation to ocean circulation. *J. Geophys. Res.*, **70**, 4547–4559.

——, 1981: An estimate of equatorial upwelling in the Pacific. *J. Phys. Oceanogr.*, **11**, 1205–1214.

——, and B. Kilonsky, 1984: Mean water and current structure during the Hawaii–Tahiti Shuttle Experiment. *J. Phys. Oceanogr.*, **14**, 242–254.

——, and G. Meyers, 1976: The trade wind field over the Pacific Ocean. *J. Appl. Meteor.*, **15**, 698–704.

——, L. Magaard and J. Hager, 1976: Eddy energy in the oceans. *J. Geophys. Res.*, **81**, 2641–2646.

——, G. Meyers, D. McLain and W. Patzert, 1977: Variability of the thermal structure in the central equatorial Pacific Ocean. Hawaii Inst. Geophysics Rep. HIG-77-1, University of Hawaii, 75 pp, 43 figs.